Ab Initio and DFT Investigations of the Mechanistic Pathway of Singlet Bromocarbenes Insertion into C-H Bonds of Methane and Ethane

M. Ramalingam[1], K. Ramasami[2], P. Venuvanalingam[3], and J. Swaminathan[4]

[1] Rajah Serfoji Government College, Thanjavur-613005, India
km_ramalingam@yahoo.co.in
[2] Nehru Memorial College, Puthanampatti-621007, India
[3] Bharathidasan University, Tiruchirapalli-620024, India
[4] Periyar Maniammai College of Technology for Women, Vallam–613403, India

Abstract. The mechanistic pathway of singlet bromocarbenes (^{1}CHBr and $^1CBr_2$) insertions into the C-H bonds of methane and ethane have been analysed at ab initio (HF and MP2) and DFT (B3LYP) level of theories using 6-31g (d, p) basis set. The QCISD//MP2/6-31g(d, p) level predicts higher activation barriers. NPA, Mulliken and ESP charge analyses have been carried out along the minimal reaction path by the IRC method at B3LYP and MP2 levels for these reactions. The occurrence of the TSs either in the electrophilic or nucleophilic phase and net charge flow from alkane to carbene in the TS has been identified through NBO analyses.

Keywords: bromocarbenes; ab initio; DFT,; insertions; IRC.

1 Introduction

The carbenes and halocarbenes are known as reactive intermediates with intriguing insertion, addition, and rearrangement reactions. How structural factors (bond angle, electron-withdrawal by induction and electron-donation by resonance) influence the relative stabilities of these states is still under scrutiny [1]. The synthetic organic chemistry [2], organometallic chemistry [3] and other areas, principally; the Arndt-Eistert chain homologation procedure, the Rimer-Tiemann reaction (formylation of phenols), cyclopropanation of alkenes [4] and subsequent rearrangements, [5] ketene and allene [6] preparation, synthesis of strained ring systems, ylide generation and subsequent rearrangements, cycloaddition reactions [7] and photoaffinity labeling. [8] are some of the vital fields of wide applications of the carbenes and halocarbenes

Among the different types of reactions of singlet carbenes, the highly characteristic concerted insertion reactions into Y-H bonds (Y=C, Si, O etc.), involving a three-center cyclic transition state [9] seem to be important in synthetic organic chemistry [2]. In the halocarbenes, the halogens would interact with the carbenic carbon through the oppositely operating electronic [mesomeric (+M) - π donor and inductive (-I) - σ acceptor] effects. Based on this, the electrophilicity of carbenes has been reported to

Y. Shi et al. (Eds.): ICCS 2007, Part II, LNCS 4488, pp. 288–295, 2007.

decrease with increased bromination resulting in a substantially high activation barrier [10]. Interestingly both the electrophilicity and nucleophilicity nature of carbenes have been encountered in the insertion reactions [11]. Hence the focal theme of this investigation is the characterization of these two features in terms of the quantum of charge transfer among the reactants during the course of the reaction and to determine the energetics, reaction enthalpies and activation barriers for the singlet bromocarbenes insertion reactions into C-H bonds of methane and ethane. If we monitor the total charge on the carbene moiety as the reaction progresses (by following, the Intrinsic Reaction Coordinate -IRC [12]) we should be able to detect a "turning point", signifying the end of the first electrophilic phase and the onset of the second nucleophilic phase. In order to properly confirm the two-phase mechanism, we carry out the charge versus reaction path probe for the insertion reactions into C-H bonds of said alkanes. In this study we investigate the reactions CBrX + HY with X = H, Br and Y = CH_3, C_2H_5. The rapidity of carbene reactions has challenged experimental techniques and hence this theoretical ab initio quantum mechanical investigations.

2 Computational Details

Geometries of the reactants, the transition states and the products have been optimized first at HF/6-31g (d, p) level using Gaussian03W suite of program [13]. The resultant HF geometries obtained were then optimized at MP2 and B3LYP [14-18] levels. The standard 6-31g (d, p) [19, 20] basis set has been adopted in all the calculations for better treatment of 1, 2-hydrogen shift during the insertion process. Further single point energy calculations have been done at the QCISD level on the MP2 optimized geometries of the species on the lowest energy reaction pathway.[21] All the stationary points found, except those obtained at the QCISD level, were characterized as either minima or transition states (TSs) by computing the vibrational harmonic frequencies – TSs have a Hessian index of one while minima have zero hessian index. All TSs were further characterized by animating the imaginary frequency in MOLDEN [22] and by checking with intrinsic reaction coordinate (IRC) analyses. The calculated vibrational frequencies have been used to compute the thermodynamic parameters like enthalpies of the reaction. The intrinsic reaction coordinate analyses have been done for the transition structures obtained at the MP2 level [23]. The Mulliken [24], NPA [25] and charges derived by fitting the electrostatic potential [26] methods have been followed for the atomic charges computations, along the reaction path.

3 Results and Discussion

The C-H bonds of methane and ethane undergo insertion reactions with $^1CHBr/^1CBr_2$ forming mono/dibromoalkanes. Reactants first form a pre-reactive complex. The complex proceeds to form a concerted transition state that then develops into a

product. The energy profile diagram for the insertion reactions of ^{1}CHBr and $^1CBr_2$ into methane is shown in Fig. 1, in which the energies of complex, transition state and the product are shown with reference to the reactants.

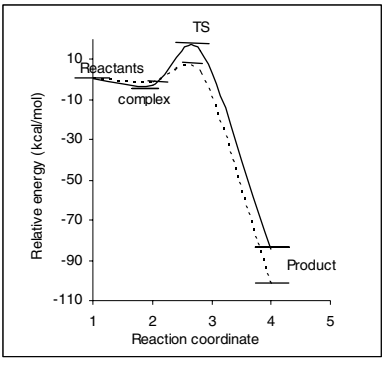

Fig. 1.

- - - - - Energy profile for ^{1}CHBr + CH_4 → CH_3-CH_2Br at MP2/6-31g**
——— Energy profile for $^1CBr_2$ + CH_4 → CH3-$CHBr_2$ at MP2/6-31g**

The optimized geometries of the TSs located in the reaction pathway for ^{1}CHBr and $^1CBr_2$ insertion reactions are presented in Fig. 2.

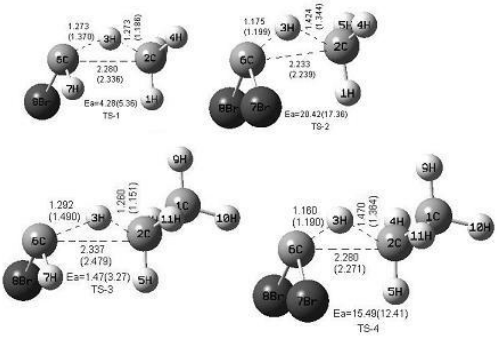

Fig. 2. Geometrical parameters (distance in Å) and barriers of the transition states for CHBr and CBr_2 insertion into C-H bond of methane and ethane at B3LYP and MP2 levels. (MP2 values in the parentheses).

3.1 Singlet Bromocarbenes Insertion into Methane and Ethane

The B3LYP, MP2 and QCISD results alone have been taken for discussions in this investigation since HF overestimates the transition states [27, 28]. The B3LYP/6-31g (d, p) activation energies for the insertions of ^{1}CHBr and $^1CBr_2$ into C-H of methane

are 4.28(TS-1) and 20.42 (TS-2) kcal/mol respectively. The MP2 value for ^{1}CHBr insertion is *ca.* 1 kcal/mol higher and that for $^1CBr_2$ insertion is *ca.* 3 kcal/mol lower than those of the corresponding B3LYP values. Replacement of hydrogen by bromine in ^{1}CHBr decreases its electrophilicity [29], and deactivates the electrophilic attack to certain extent by the carbene moiety in the first phase of insertion. So the barrier heights increase dramatically from 4.28 to 20.42 kcal/mol at B3LYP and 5.36 to 17.36 kcal/mol at MP2 calculations respectively for methane. The barriers computed at QCISD/6-31g (d, p)//MP2/6-31g (d, p) level are 9.68 kcal/mol and 23.93 kcal/mol for ^{1}CHBr and $^1CBr_2$ insertion into methane. The TSs are first order saddle points as determined by numerical vibrational frequency.

In the case of ethane, the barrier heights for ^{1}CHBr insertion are 1.47 and 3.27 kcal/mol respectively at B3LYP and MP2 levels (TS-3). These values have been enhanced to 15.49 and 12.41 kcal/mol (TS-4) correspondingly for the $^1CBr_2$ insertion. The relevant geometrical parameters of the transition states for the ^{1}CHBr and $^1CBr_2$ insertions to methane and ethane have been shown in Fig. 2, Table 1 and 2. The TS for $^1CBr_2$ insertion into methane (TS-2) comes much later along the reaction coordinate than that for ^{1}CHBr insertion (TS-1) as reflected in the relative C2-H3 bond distances of 1.430 (1.345) and 1.274 (1.202) Å and the charges on H3, 0.279(0.278) and 0.255 (0.216) respectively. Similar trend has been observed for the singlet bromocarbenes insertion into ethane.

Table 1. Geometrical parameters (distances in Å), barriers and heat of reaction (ΔHr) in kcal/mol at the TSs of ^{1}CHBr with alkanes at B3LYP (MP2)/6-31g (d, p)

alkane	r_{c1h1}	r_{c1c2}	r_{c2h1}	Ea	q_{ct}	ΔHr
methane	1.276	22.280	1.273	4.28	0.252	-87.41
	(1.370)	((2.336)	(1.186)	(5.36)	(0.187)	(-96.40)
ethane	1.292	2.337	1.260	1.47	0.267	-89.13
	(1.490)	(2.479)	(1.151)	(3.27)	(0.130)	(-99.31)

q_{ct} – quantum of charge transfer from alkane to carbene at the TSs

Table 2. Geometrical parameters (distances in Å), barriers and heat of reaction (ΔHr) in kcal/mol at the TSs of $^1CBr_2$ with alkanes at B3LYP (MP2)/6-31g (d, p)

alkane	r_{c1h1}	r_{c1c2}	r_{c2h1}	Ea	q_{ct}	ΔHr
methane	1.175	22.233	1.424	20.42	0.322	-68.95
	(1.199)	(2.239)	(1.344)	(17.36)	(0.382)	(-80.85)
ethane	1.160	2.280	1.470	15.49	0.362	-71.27
	(1.190)	(2.271)	(1.364)	(1(2.41)	(0.402)	(-84.86)

q_{ct} – quantum of charge transfer from alkane to carbene at the TSs

3.2 Energetics

In general the activation barrier depends upon the polarity of the C-H bond of alkane and the type of bromocarbene (^{1}CHBr or $^1CBr_2$) to be inserted. The above statement draws support from the fact that the pair of electrons on the carbene carbon involved in the bonding process with the C-H of alkane is more and more stabilized with the degree of bromination. This results in the inhibition of the ease of bond formation due to the less availability of the electron pair on the cabene carbon. The NBO [30] analysis quantifies this aspect in terms of the energies of the electron pairs on ^{1}CHBr and $^1CBr_2$ as -0.4057(-0.5595) and -0.4535 (-0.6019) au respectively according to B3LYP (MP2) theories with 6-31g (d, p) basis set. The enthalpies of the insertion reactions of ^{1}CHBr and $^1CBr_2$ into methane are -87.41(-96.40) and –68.95(-80.85) and that for ethane are –89.31(-99.31) and –71.27(-84.86) kcal/mol at B3LYP (MP2) levels respectively. The reaction enthalpies (Tables 1 and 2) show that the exothermicity of the insertion reactions indicating that the transition states analyzed resemble the reactants rather than the products [31]. The proximity of the transition states to the reactants deviates with the degree of bromination of methylene. Irrespective of the level of theory (B3LYP or MP2) followed, the insertions of ^{1}CHBr form the transition states earlier than that of $^1CBr_2$ as revealed by exothermicity values.

3.3 Transition State Geometries

A scrutiny of the bond breaking and bond forming steps corresponding to C2-H3 and C6-H3 respectively during the insertion process reveals that it is a concerted reaction. It is observed that the formation of C6-H3 bond is earlier than the C2-C6 bond in the TS in terms of the bond distances (Tables 1 and 2). The C6-H3, C2-H3 and C2-C6 bond distances in TSs of $^1CBr_2$ insertion reactions confirm the late transition state in comparison to the corresponding values in the ^{1}CHBr insertion reactions. In order to improve the accuracy of the energetic parameters, single point computations at QCISD level has also been adopted and values are listed in Tables 1and 2. The barrier heights predicted at QCISD level are higher than the MP2 values both for methane and ethane.

3.4 NBO Analyses

NBO analyses of charge distribution in the transition states give some insight into the insertion reactivity. For all the transition states the second-order perturbative analyses were carried out for all possible interactions between filled Lewis-type NBOs and empty non-Lewis NBOs. These analyses show that the interaction between the σC2-H3 bond of alkane and the empty p_π orbital of the carbenic carbon ($\sigma_{CH} \rightarrow P_C$) and the charge transfer from lone pair of electrons of the carbenic carbon to the antibonding orbital of C2-H1($n_C \rightarrow \sigma^*_{CH}$) seems to give the strongest stabilization. Finally we observed that there was a net charge flow from the alkane moiety to the inserting carbene moiety. The quantum of charge transfer from alkane to carbene supporting the donor-acceptor interaction in the transition states for all the insertion reactions both at B3LYP and MP2 levels have been collected in Tables 1 and 2. The

inverse relationship between the quantum of charge transfer and the activation barriers reveals the fact that for the favorable insertion, the nucleophilicity of the alkane should have been enhanced either sterically or electronically. This correlation holds good for the reactions analysed in this investigation

3.5 IRC - Charge Analyses

The total charge on the carbene moiety along the IRC for the insertion reactions of methane and ethane respectively, as calculated by Mulliken [23], NPA [24] and ESP [25] methods using theoretical models has been shown in Fig.3. We have chosen density functional (B3LYP) plot showing charge on the carbene moiety in addition to the MP2 plot, which serve as our ab initio "standard".

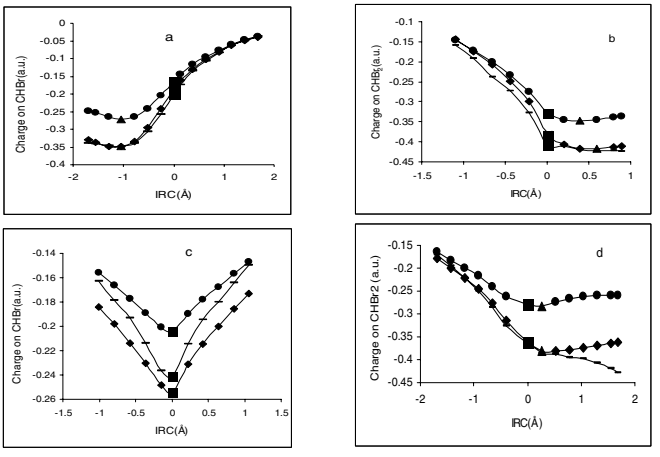

Fig. 3. (♦)-NPA, (●)-Mulliken and (-)-ESP charge analyses respectively. (■) and (▲) correspond to the transition states and the turning points respectively. Electrophilic-phase region – right to the turning point Nucleophilic-phase region – left to the turning point.

We discuss first the insertion reactions with methane, ^{1}CBrX (X = H, Br) + CH4. The charge/IRC curves of these reactions are shown in Figs. 3. These two reactions provide clear evidence for the two-phase mechanism in that there is a distinct turning point(minimum) in all the charge/IRC curves for the two Hamiltonians (MP2 and B3LYP) regardless of the model used to compute the atomic charges. For the ^{1}CHBr insertion (Fig.3 a), the charge minimum occurs after the transition state (TS), whereas with $^1CBr_2$ (Fig. 3b) the minimum occurs just before the TS. Thus for the ^{1}CHBr insertion, the TS lies within the first, i.e., electrophilic phase, whereas for $^1CBr_2$ the TS is reached at the starting point of the nucleophilic phase. This indicates that the TS for insertion of ^{1}CHBr into the C-H bond in methane occurs much earlier along the reaction coordinate than does the TS for the corresponding $^1CBr_2$ insertion. This indication is fully supported both by the TS geometries - for example, the C-H bond undergoing the insertion is much shorter in the ^{1}CHBr (1.202Å) TS than in the TS for $^1CBr_2$ (1.345Å) insertion (Fig. 2) and by the heat of reaction and barrier height

(Tables 1 and 2), which are more negative and much smaller, respectively for ^{1}CHBr (-96.40; 5.36kcal/mol respectively) than for $^1CBr_2$. (-80.85; 17.36 kcal/mol respectively). This is in agreement with the Hammond postulate [32]. From the viewpoint of reactivity, it may be said that the vacant p-orbital on ^{1}CHBr is more available than that on $^1CBr_2$, thus facilitating the initial electrophilic phase of the reaction. In other words, reactivity increases in the order $^1CBr_2 < {}^1$CHBr. There is an agreement in the overall shape and "depth" of the curves themselves between the MP2 and B3LYP plots. However the turning points (minima) in the B3LYP plots are less pronounced. The NPA and ESP curves are identical in shape at MP2 level.

In the case of ethane, ^{1}CBrX (X = H, Br) + C_2H_6 the position of the turning points and the charge/IRC curves for these insertions at MP2 level are shown in (Fig. 3). Unlike for the ^{1}CHBr insertion into methane, the TS-3 occurs at the turning point (Fig. 1c), which is in neither electrophilic phase nor nucleophilic phase. But for $^1CBr_2$ insertion into ethane at MP2 (Fig. 1d), the TS is observed at the starting point of the nucleophilic phase conforming to the belated TS formation in comparison with the TS for insertion of ^{1}CHBr (Fig. 1c). In general, the nucleophilic phase dominates for $^1CBr_2$ insertions, whereas the electrophilic phase dominates ^{1}CHBr insertions.

4 Summary

The singlet bromocarbenes insertions into the C-H bond of methane and ethane have been analyzed and the influence of bromine on the transition states, energetics, geometrical parameters etc., has been investigated both at B3LYP and MP2 levels of theory using 6-31g (d, p) basis set. For the bromocarbenes B3LYP, MP2 and QCISD level theories predict the activation barriers of different heights, varying both with the extent of bromination and the type of alkane. The NBO analyses have been done with a view to analyzing the charge transfer processes during the insertion reactions. The charge/IRC plots provide clear evidences for the two-phase mechanism namely an electrophilic phase and a nucleophilic phase for insertions of both ^{1}CHBr and $^1CBr_2$ into the C-H bond of methane and ethane respectively. B3LYP functional used in this work, gives the same "picture" of the investigated insertion reactions as the more traditional MP2 method for both geometries and heats of reaction.

References

1. Irikura, K, K., Goddard, W.A., Beauchamp, J.L.: J.Am.Chem.Soc. 114 (1992) 48
2. Kirmse, W.: Carbene Chemistry. 2nd Edn. Academic Press, New York (1971)
3. Fischer, E.O., Maasbol, A.: Angew. Chem., Int. Ed. Engl. 3 (1964) 580
4. Salaun, J.: Chem. Rev. 89 (1989) 1247
5. Brookhart, M., Studabaker, W.B.: Chem. Rev. 87 (1987) 411
6. Walbrick, J. M., Wilson, J.W., Jones, W.M.: J. Am. Chem. Soc. 90 (1968) 2895
7. Padwa, A., Hornbuckle, S.F.: Chem. Rev. 91 (1991) 263
8. Baldvin, J.E., Jesudason, C.D., Moloney, M., Morgan, D.R., Pratt, A.J.: Tetrahedron 47 (1991) 5603
9. Von, W., Doering, E., Prinzbach, H.: Tetrahedron 6 (1959) 24
10. Russon, N., Siclia, E., Toscano, M.: J. Chem. Phys. 97 (1992) 5031

11. Dobson, R.C., Hayes, D.M., Hoffmann, R.: J. Am.Chem. Soc. 93 (1971) 6188
12. Fukui, K.: J. Phys. Chem. 74 (1970) 4161
13. Gaussian 03, Revision C.02, Gaussian, Inc., Wallingford CT (2004)
14. Lee, C., Yang, W., Parr, R.G.: Physical Review B 37 (1988) 785
15. Becke, D.: Phys. Rev. A 38 (1988) 3098
16. Miehlich, B., Savin, A., Stoll, H., Preuss, H.: Chem. Phys. Lett. 157 (1989) 200
17. Becke, A.D.: J. Chem. Phys. 98 (1993) 5648
18. Becke, A.D.: J. Chem. Phys. 104 (1996) 1040
19. Franel, M.M., Pietro, W.J., Hehre, W.J., Bimcley, J.S., Gordon, M.S., DeFrees, D.J., Pople, J.A.: J. Chem. Phys., 77 (1982) 3654.
20. Hariharan, P.C., Pople, J.A.: Chem. Phys. Lett. 66 (1972) 217
21. Pople, J. A., Gordon, M. H., Raghavachari, K.:.J. Chem. Phys. 87 (1987) 5968
22. Schaftenaar,G., Noordik,J.H.: J Comput Aid Mol Design 14 (2000) 123
23. Gonzalez, C., Schlegel, H.B.: J. Chem. Phys.94 (1990) 5523
24. Mulliken, R.S.: J. Chem. Phys. 23 (1955) 1833
25. Reed, A.E., Carpenter, J.E., Weinhold, F., Curtiss, L.A.: Chem. Rev. 88 (1988) 8991
26. Breneman, C.M., Wiberg, K.B.:J. Comput. Chem. 11 (1990) 361
27. Ramalingam, M., Ramasami, K., Venuvanalingam, P., Sethuraman, V.: J. Mol.Struct.(Theochem) 755 (2005) 169
28. Bach, R.D., Andres, J.L., Su, M.D., McDouall, J.J.W.: J. Am. Chem. Soc. 115 (1993) 5768
29. Gilles, M.K., Lineberger, W.C., Ervin, K.M.: J. Am. Chem. Soc.115 (1993) 1031
30. Glendening, E.D., Reed, A.E., Carpenter, J.E., Weinhold, F., Curtiss, L.: Chem. Rev. 88 (1988) 899 NB Version 3.1
31. Carpenter, J.E.: Ph.D. Thesis, University of Wisconsin (Madison, WI) (1987)
32. Hammond, G.S.: J. Am. Chem. Soc. 77 (1955) 334